Heterogeneous Catalysis

International Edition: DOI: 10.1002/anie.201605934
German Edition: DOI: 10.1002/ange.201605934

Tungsten(VI) Carbyne/Bis(carbene) Tautomerization Enabled by N-Donor SBA15 Surface Ligands: A Solid-State NMR and DFT Study

*Anissa Bendjeriou-Sedjerari, Julien Sofack-Kreutzer, Yury Minenkov, Edy Abou-Hamad, Bilel Hamzaoui, Baraa Werghi, Dalaver H. Anjum, Luigi Cavallo, Kuo-Wei Huang, and Jean-Marie Basset**

Abstract: *Designing supported well-defined bis(carbene) complexes remains a key challenge in heterogeneous catalysis. The reaction of W(≡C*t*Bu)(CH_2*t*Bu)$_3$ with amine-modified mesoporous SBA15 silica, which has vicinal silanol/silylamine pairs [(≡SiOH)(≡$SiNH_2$)], leads to [(≡$SiNH_2$–)(≡SiO–)W(≡CH*t*Bu)(CH_2*t*Bu)$_2$] and [(≡$SiNH_2$–)(≡SiO–)W(=CH*t*Bu)$_2$(CH_2*t*Bu). Variable temperature, ^{1}H–^{1}H 2D double-quantum, ^{1}H–^{13}C HETCOR, and HETCOR with spin diffusion solid-state NMR spectroscopy demonstrate tautomerization between the alkyl alkylidyne and the bis(alkylidene) on the SBA15 surface. Such equilibrium is possible through the coordination of W to the surface [(≡Si–OH)(≡Si–NH_2)] groups, which act as a [N,O] pincer ligand. DFT calculations provide a rationalization for the surface–complex tautomerization and support the experimental results. This direct observation of such a process shows the strong similarity between molecular mechanisms in homogeneous and heterogeneous catalysis. In propane metathesis (at 150°C), the tungsten bis(carbene) tautomer is favorable, with a turnover number (TON) of 262. It is the highest TON among all the tungsten alkyl-supported catalysts.*

One of the objectives of surface organometallic chemistry is to transfer the concepts of molecular chemistry to surface chemistry.[1] The main strategy is to use surface organometallic fragments (SOMF) to enter directly into the catalytic cycle of a given reaction, leading to real predictive catalysis by design.[1b] Through this approach, we proposed, for example, that olefin metathesis should require a surface metallocarbene and alkane metathesis should require a metallocarbene hydride or a metallocarbene alkyl.[1b,2] In the past, we reported the grafting of W(≡C*t*Bu)(CH_2*t*Bu)$_3$ (**1**) on a partially dehydroxylated silica surface (at 700°C) to yield the monopodal species: [≡Si–O–W(≡C*t*Bu)(CH_2*t*Bu)$_2$].[3] This carbyne was found to be inactive in propane metathesis[1b,4] and active in propene metathesis, which led to some speculation on the real mechanism. In molecular organometallic chemistry, Xue et al. discovered that an equilibrium could occur between (tBuCH$_2$)$_2$W(≡C*t*Bu)(Si*t*BuPh$_2$) and (tBuCH$_2$)–W(=CH*t*Bu)$_2$(Si*t*BuPh$_2$).[5] This tautomerization process occurs through α-hydrogen transfer from a neopentyl to the carbyne (at 287 K). Until now, such equilibrium was promoted by the coordination of sterically bulky phosphine[6] on a classical silica surface.[7] Our interest was to achieve a direct isolation and characterization of a W bis(carbene) alkyl tautomeric form as a SOMF-active metathesis carried out in propane.

Recently, we reported the synthesis of SBA15 containing adjacent ≡$SiNH_2$ and ≡Si–OH surface groups.[8] Herein, we describe the chemisorption of W(≡C*t*Bu)(CH_2*t*Bu)$_3$ on such a surface, which plays the role of chelating [N,O] pincer ligands, leading to [(≡$SiNH_2$–)(≡SiO–)W(≡CH*t*Bu)(CH_2*t*Bu)$_2$] (**3a**) and [(≡$SiNH_2$–)(≡SiO–)W(=CH*t*Bu)$_2$(CH_2*t*Bu)] (**3b**) (Scheme 1).

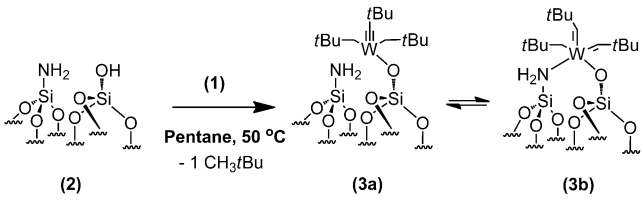

Scheme 1. Reaction of W(≡C*t*Bu)(CH_2*t*Bu)$_3$ (**1**) with a [N,O] chelating SBA15 surface (**2**).

Reaction of W(≡C*t*Bu)(CH_2*t*Bu)$_3$ (**1**) with **2**, in pentane at 50°C leads to the formation of a tungsten complex covalently bonded to silica in accordance with the gas-phase analysis (0.9 ± 0.1 equivalent of gaseous neopentane per W), a C/W ratio of 16 is consistent with the theoretical value (15) for a compound retaining 3 neopentyl-like species. Finally, W/N and C/N ratios of 0.9 and 14.3, respectively, agree with the expected value for either [(≡$SiNH_2$–)(≡SiO–)W(≡CH*t*Bu)(CH_2*t*Bu)$_2$] (**3a**) or [(≡$SiNH_2$–)(≡SiO–)W(=CH*t*Bu)$_2$(CH_2*t*Bu)] (**3b**; Supporting Information, Table S1).

The FTIR bands characteristic of the starting ≡$SiNH_2$ moiety are found at 3532 [$\upsilon_{as}(NH_2)$], 3448 [$\upsilon_s(NH_2)$], and 1550 cm^{-1} [$\delta(NH_2)$]. After reaction of **1** with **2**, a total consumption of isolated silanols [υ(OH) at 3741 cm^{-1}] is observed. In contrast, the characteristic bands of the silylamine groups are still present but with a slight blue shift (−5 cm^{-1}) at 3527 and 3442 for $\upsilon_{as}(NH_2)$ and $\upsilon_s(NH_2)$, respectively (Figure 1). Notably, a weak consumption of the characteristic vibration bands of the silylamine group, $\upsilon_{as}(NH_2)$ and $\upsilon_s(NH_2)$, is observed in accordance with the presence of the weak υ(NH) stretching bands at 3226 and

[*] A. Bendjeriou-Sedjerari, J. Sofack-Kreutzer, Y. Minenkov, E. Abou-Hamad, B. Hamzaoui, B. Werghi, D. H. Anjum, L. Cavallo, K. W. Huang, J. M. Basset
King Abdullah University of Science and Technology (KAUST)
Kaust Catalysis Center (KCC)
Thuwal, 23955-6900 (Saudi Arabia)
E-mail: jeanmarie.basset@kaust.edu.sa

Supporting information for this article can be found under: http://dx.doi.org/10.1002/anie.201605934.

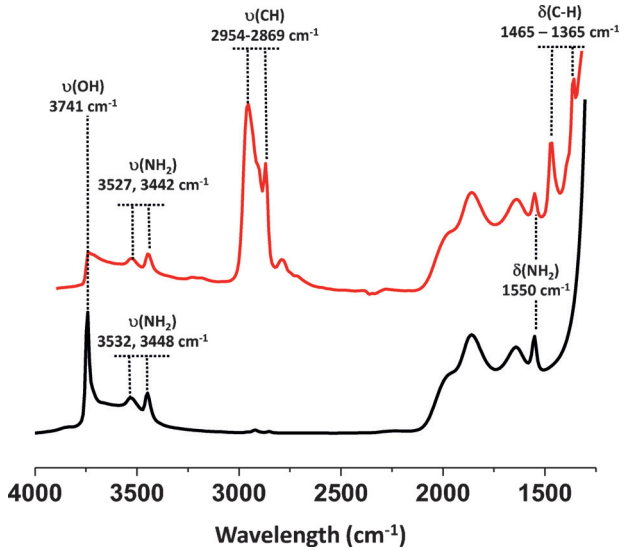

Figure 1. FTIR spectra of **2** in black and **3** in red.

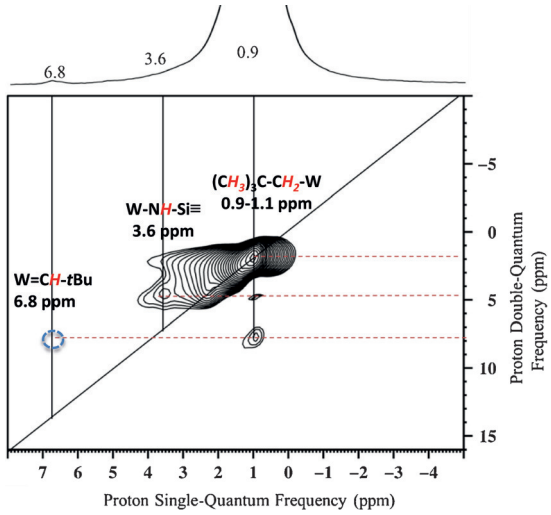

Figure 2. ^{1}H–^{1}H double-quantum (DQ)/single-quantum (SQ) NMR spectrum of **3** (acquired at 600 MHz with a 22 kHz MAS frequency, 32 scans per t_1 increment, 5 s repetition delay, and 128 individual t_1 increments).

3180 cm^{-1} (Supporting Information, Figure S3 and Scheme S1).[8a,9] This observation is consistent with the formation of a small amount (< 10 %) of a covalent bond between the NH surface ligand and W.

The coordination sphere of the tungsten species in **3** was elucidated by various solid-state NMR studies. The ^{1}H NMR spectrum of **3** displays two intense signals at 0.9 and 1.1 ppm assigned to the remaining neopentyl-like group (CH_2 and CH_3). A weak signal at 2 ppm could be tentatively attributed to $\equiv SiNH_2$ coordinated to W (Supporting Information, Figure S4).[10] Interestingly, the spectrum exhibits also a weak signal at 6.8 ppm, which could be assigned to the proton of a carbene (Figure 2 and the Supporting Information, S4 enlargement).[5a]

2D ^{1}H–^{1}H double-quantum (DQ) solid-state NMR spectroscopy was performed to investigate the probable and rare transformation of the d^0-alkyl-alkylidyne (**3a**) to its alkylidene tautomer (**3b**) upon grafting of **1**. The DQ spectrum of **3** shows a strong auto-correlation peak on the 2:1 diagonal centered at around 0.9 ppm in F2 and at 1.8 ppm in F1 (Figure 2). These resonances are assigned to the CH_2 and CH_3 moieties. The proton resonance at 0.9 ppm shows a weak correlation with the proton at 3.6 ppm assigned to ≡Si–NH–W [4.5 ppm in F1: $\delta H(CH_3/CH_2) + \delta H(NH) = 0.9 + 3.6$] establishing the identity of the minor species (Supporting Information, Scheme S1, **3c** and **3d** ca. 10 %). Furthermore, the correlation at about 7.7 ppm corresponds to [$\delta H(CH_3) + \delta H(W{=}CH) = 0.9 + 6.8$], which confirms the presence of the bis(alkylidene) (**3b**).

To unambiguously confirm these results, ^{13}C cross-polarization magic-angle spinning (CP-MAS) and ^{1}H–^{13}C two-dimensional (2D) heteronuclear correlation (HETCOR) with short contact times (0.2 ms) and ^{1}H–^{13}C HETCOR with spin diffusion using a long mixing time ($\tau_m = 100$ ms) experiments were performed.

The ^{13}C CP-MAS spectrum of **3** reveals a clear pattern, as six signals are identified (Figure 3). As observed previously, the spectrum has signals at 32, 51, and 95 ppm assigned to the [W–$CH_2C(CH_3)_3$], [W–CH_2CH_3], and [W–$CH_2C(CH_3)_3$], respectively. Note that additional signals are observed at 30 and 316 ppm, which can be assigned to [W≡C–$C(CH_3)_3$] and [W≡C–$C(CH_3)_3$], respectively, by comparison with the ^{13}C NMR spectrum of **2** in solution in deuterated benzene (Supporting Information, Figure S2). Additionally, the presence of a resonance at 227 ppm confirms the presence

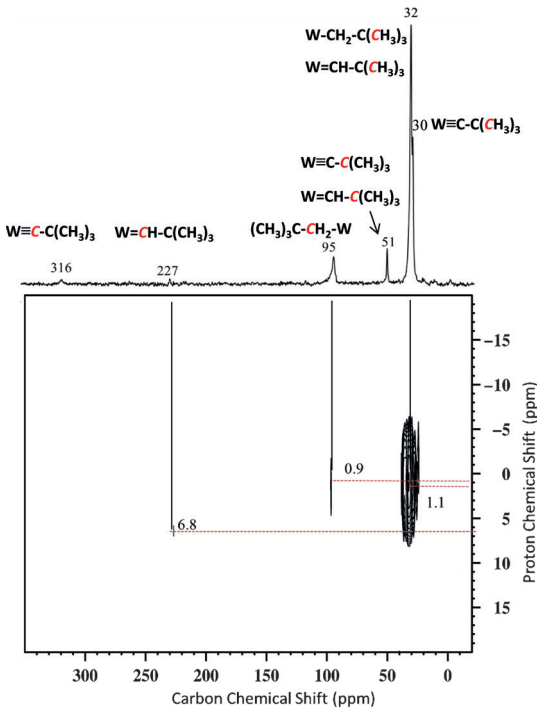

Figure 3. Two-dimensional ^{1}H–^{13}C CP/MAS dipolar HETCOR spectrum of **3** (acquired at 600 MHz proton frequency with an 8.5 kHz frequency, 4000 scans per t_1 increment, a 4 s repetition delay, 32 individual t_1 increments, and a 0.2 ms contact time).

of metallocarbene species, [W=*C*H–C(CH_3)$_3$]. These results unambiguously confirm the presence of a supported tungsten d^0-alkyl alkylidyne and a bis(alkylidene). The ^{1}H–^{13}C HETCOR spectrum of **3** revealed, as expected, a correlation between the alkylidene carbon resonance at 227 ppm and its proton resonance at 6.8 ppm (Figure 3). Furthermore, a cross-peak between the alkylidyne carbon at 316 ppm and the proton of the alkylidene at 6.8 ppm was clearly observed in the ^{1}H–^{13}C dipolar HETCOR with ^{1}H spin diffusion period (Figure 4), resulting from a chemical exchange process between **3a** and **3b**.

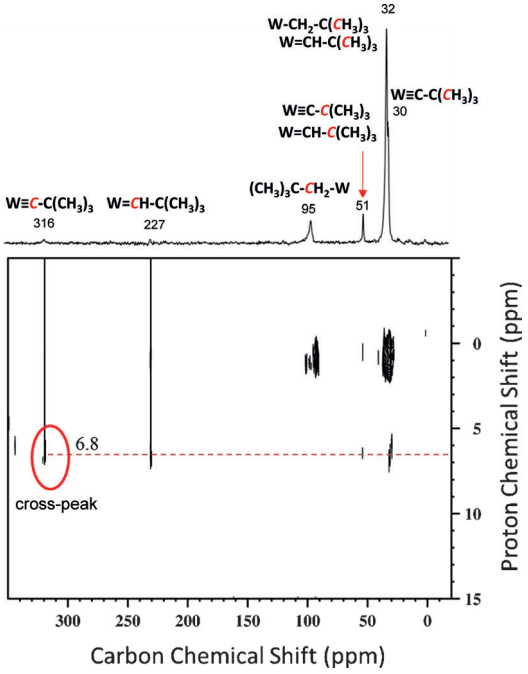

Figure 4. Two-dimensional ^{1}H–^{13}C spin diffusion HETCOR spectrum of **3** (acquired at 600 MHz proton frequency with an 8.5 kHz frequency, 4000 scans per t_1 increment, a 4 s repetition delay, 64 individual t_1 increments, and a mixing time $\tau_m = 100$ ms).

Finally, variable-temperature ^{1}H solid state NMR studies highlight the isomerization of **3a** to **3b** (Figure 5). Thus, decreasing the temperature to 230 K results in the total disappearance of the neopentylidene proton resonance observed at 6.8 ppm at 300 K. In contrast, the same resonance reappears with a higher intensity at 340 K, which indicates that the neopentylidene tautomer **3b** is favored at high temperatures. At this temperature, the broad signal of the corresponding carbene is split. This suggests that both *syn* and *anti* isomers exist (Supporting Information, Scheme S2), indicative of the rigid behavior of the two carbenes.[5a,d,6b,11] Furthermore, the proton signal at 2 ppm (previously assigned to the ≡Si–NH_2 group coordinated to W) is more intense at 340 K, supporting the effect of coordination between N and W atoms at high temperatures. This tendency is similar to what was observed by Xue et al.[5] in molecular chemistry, which shows the benefit of SOMC in transferring the concepts of molecular chemistry to surface chemistry.

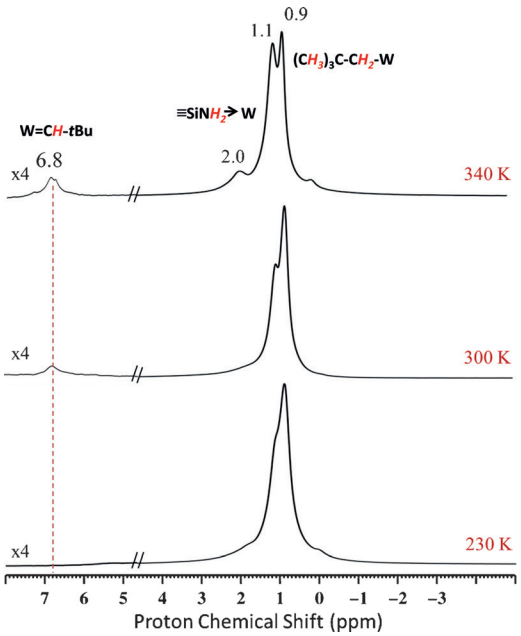

Figure 5. Variable temperature ^{1}H MAS NMR spectra of **3** (acquired at 600 MHz with a 15 kHz MAS frequency, a repetition delay of 5 s, and 8 scans).

To understand these results, we performed density functional theory (DFT) calculations (see the Supporting Information for computational details). We examined the **3a″**⇌**3b″** equilibrium in the absence of the ≡Si–NH_2 group, that is, on an unmodified silica surface dehydroxylated at 200 °C (Supporting Information, Figure S8). Practically all the tested functionals predict the tungsten bis(neopentylidene) (**3b′**) to be higher in Gibbs free energy compared to the neopentyl-neopentylidyne tautomer (**3a′**) by approximately 5–6 kcal mol^{-1}, except for the M06 functional, which predicts **3a′** to be more stable by 8 kcal mol^{-1}. This underlines that the equilibrium between the two tautomers on the classical silica surface (SiO_{2-200}), is strongly shifted towards the formation of the neopentyl-neopentylidyne tungsten (**3a′**). This is in accordance with the experimental evidence that the bis(neopentylidene) species (**3b′**) is not detected by NMR after reaction of tungsten tris-neopentyl-neopentylidyne on both classical SiO_{2-200} and SiO_{2-700} surfaces.[3] The activation Gibbs free-energy barrier associated with the tautomerization of **3a′** to **3b′** is quite high, approximately 27 kcal mol^{-1}, to be overcome at room temperature (Table 1).

Next, we focused on examining the impact of a vicinal ≡Si–NH_2 group on the **3a**⇌**3b** equilibrium. The first question we addressed is the eventual coordination of the ≡Si–NH_2 group to the W atom. To this end, we performed a conformational search (see the Supporting Information), which indicated that for **3a**, the most stable structure does not show a ≡Si–NH_2···W interaction (W–N distance of 3.85 Å) (Figure 6).

Indeed, the most stable structure of **3a** involving the formation of a W–NH_2 bond (a W–N distance of ca. 2.6 Å) is about 3 kcal mol^{-1} higher in energy. Conversely, the most stable structure of the **3b** tautomer shows the NH_2 group coordinated to tungsten atom (W–N distance of 2.63 Å). This

Table 1: Activation and standard Gibbs free energy [kcal mol^{-1}] calculated for the equilibrium between tungsten neopentylidyne and its bis(neopentylidene) tautomer on classical (**3a′**⇌**3b′**) and amine-modified (**3a**⇌**3b**) silica surfaces at room temperature.

	TPSS-D3	TPSSh-D3	PBE-D3	PBE0-D3	M06
Thermochemistry					
ΔG(**3a′**/**3b′**)	5.1	5.4	5.1	5.9	8.3
ΔG(**3a**/**3b**)	2.5	3.3	4.2	5.3	6.3
$\Delta\Delta G$	−2.6	−2.1	−0.9	−0.6	−2.0
Activation					
ΔG^{+}(**3a′**/**3b′**)	26.7	27.8	25.5	28.6	31.1
ΔG^{+}(**3a**/**3b**)	24.2	25.5	23.1	26.5	28.4
$\Delta\Delta G^{+}$	−2.5	−2.3	−2.4	−2.1	−2.7

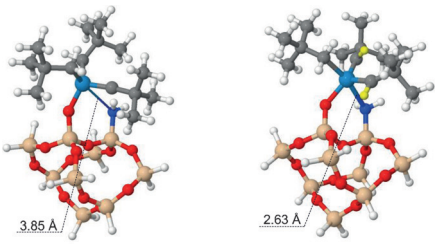

Figure 6. Calculated geometries of [(≡SiNH$_2$−)(≡SiO−)W(≡CH*t*Bu)(CH$_2$*t*Bu)$_2$] (**3a**) and of [(≡SiNH$_2$−)(≡SiO−)W(≡CH*t*Bu)$_2$(CH$_2$*t*Bu)] (**3b**). Distances (N–W) are given in Å. Si beige, O red, H white, W blue, N dark blue, C gray, alkylidene H in **3b** yellow.

finding is in agreement with a previous study, which focused on the influence of PMe_3 on a similar tautomerization equilibrium in a W–bis(alkylidene) complex, in molecular organometallic chemistry.[6a]

In presence of the ≡Si–NH$_2$ group all of the tested functionals reduce the Gibbs free-energy difference between species **3b** and **3a** by roughly 1–2 kcal mol^{-1}. Incidentally, the enthalpic difference is reduced even more by the TPSS-D3 functional (by ca. 4 kcal mol^{-1}), which results in **3b** being enthalpically more stable than **3a** by 1.4 kcal mol^{-1} (see the Supporting Information). This indicates that the interaction of the ≡Si–NH$_2$ group with the W atom stabilizes **3b** more than **3a**. The evidence that entropy effects destabilize **3b** relative to **3a** is consistent with the more ordered structure of **3b**, due to the coordination of the ≡Si–NH$_2$ group to the W atom. Finally, all the functionals tested predict the Gibbs free energy barrier for the **3a**→**3b** rearrangement to be roughly 2 kcal mol^{-1} lower in presence of the ≡Si–NH$_2$ group.

The results above allow us to interpret the temperature dependence highlighted by the variable-temperature ^{1}H solid-state NMR spectroscopy (Figure 5). At low temperature (230 K), the barrier for the α-hydrogen transfer to form species **3b** cannot be overcome. Therefore, only tautomer **3a** exists on the [N,O] SBA15 surface. As the N–W interaction is lost in the most stable structure of **3a**, the corresponding resonance at 2 ppm (≡Si–NH$_2$→W) is not present in the NMR spectrum. At 300 K the surface complex **3b** appears, resulting in the presence of the signal corresponding to [W=C***H***–C(CH$_3$)$_3$], but species **3a** still dominates the surface, and the [≡Si–NH$_2$→W] signal is weak. This trend is enhanced at 340 K, with a more rapid interconversion between **3a** and **3b**, a more intense signal corresponding to [W=C***H***–C(CH$_3$)$_3$], and the clearly visible characteristic broad signal of (≡Si–NH$_2$→W).

The catalytic performance of the tungsten bis(carbene) alkyl (**3**) was evaluated in propane metathesis at 150 °C (in a batch reactor). In previous studies, the tungsten carbyne supported on silica [(≡Si–O–)W(≡C*t*Bu)(CH$_2$*t*Bu)$_2$] was inactive in propane metathesis, and the highest TON (121) was obtained on tungsten hydride supported on silica–alumina after 120 h.[4] As demonstrated by SS NMR spectroscopy and DFT calculations, the tungsten bis(carbene) neopentyl tautomer is, at this temperature, favored. Consequently, the catalytic results show that the tungsten bis(carbene) neopentyl is efficient in the conversion of propane into methane (1.6 %), ethane (60 %), butane (21 %), isobutane (8 %), and pentane (3 %) with a TON of 197 after 24 h and 262 with 26 % conversion after 240 h.

In conclusion, a direct observation of α-H exchange between alkyl alkylidyne and a bis(alkylidene) was made, which is an exciting step toward understanding the elementary steps in heterogeneous catalysis. It is interesting to note that SOMC applied to [N,O] SBA15 surfaces plays an important role in the stabilization of a tungsten bis(neopentylidene). Indeed, the formation of the tungsten bis(carbene) alkyl, favored at high temperatures on a [N,O] SBA15 surface, leads to better catalytic activity in propane metathesis compared to the classical silica-supported tungsten carbyne bis(alkyl). The fact that a surface may play the role of an external ligand for this transformation is novel and shows the power of the surface organometallic chemistry concept.

Acknowledgements

This work received support from the King Abdullah University of Science and Technology (KAUST) Office of Sponsored Research (OSR) under Award No. CRG_R2_13_BASS_KAUST_1.

Keywords: chelating ligands · α-H exchange · SBA15 silica · surface organometallic chemistry · tautomerization

How to cite: *Angew. Chem. Int. Ed.* **2016**, *55*, 11162–11166
Angew. Chem. **2016**, *128*, 11328–11332

[1] a) J. M. Basset, R. Psaro, D. Roberto, R. Ugo in *Modern surface organometallic chemistry*, Wiley-VCH, Weinheim, **2009**; hardback; b) J. D. A. Pelletier, J.-M. Basset, *Acc. Chem. Res.* **2016**, *49*, 664–677; c) C. Copéret, A. Comas-Vives, M. P. Conley, D. P. Estes, A. Fedorov, V. Mougel, H. Nagae, F. Núñez-Zarur, P. A. Zhizhko, *Chem. Rev.* **2016**, *116*, 323–421; d) P. Serna, B. C. Gates, *Acc. Chem. Res.* **2014**, *47*, 2612–2620; e) R. Anwander, *Chem. Mater.* **2001**, *13*, 4419–4438.

[2] a) N. Popoff, E. Mazoyer, J. Pelletier, R. M. Gauvin, M. Taoufik, *Chem. Soc. Rev.* **2013**, *42*, 9035–9054; b) C. Copéret, M. Chabanas, R. P. Saint-Arroman, J.-M. Basset, *Angew. Chem. Int. Ed.* **2003**, *42*, 156–181; *Angew. Chem.* **2003**, *115*, 164–191; c) P. Sautet, F. Delbecq, *Chem. Rev.* **2010**, *110*, 1788–1806.

[3] E. Le Roux, M. Taoufik, M. Chabanas, D. Alcor, A. Baudouin, C. Copéret, J. Thivolle-Cazat, J.-M. Basset, A. Lesage, S. Hediger, L. Emsley, *Organometallics* **2005**, *24*, 4274 – 4279.
[4] a) E. Le Roux, M. Taoufik, C. Copéret, A. de Mallmann, J. Thivolle-Cazat, J.-M. Basset, B. M. Maunders, G. J. Sunley, *Angew. Chem. Int. Ed.* **2005**, *44*, 6755 – 6758; *Angew. Chem.* **2005**, *117*, 6913 – 6916; b) E. Le Roux, M. Taoufik, A. Baudouin, C. Copéret, J. Thivolle-Cazat, J.-M. Basset, B. M. Maunders, G. J. Sunley, *Adv. Synth. Catal.* **2007**, *349*, 231 – 237.
[5] a) T. Chen, Z. Wu, L. Li, K. R. Sorasaenee, J. B. Diminnie, H. Pan, I. A. Guzei, A. L. Rheingold, Z. Xue, *J. Am. Chem. Soc.* **1998**, *120*, 13519 – 13520; b) S.-H. Choi, Z. Lin, Z. Xue, *Organometallics* **1999**, *18*, 5488 – 5495; c) K. G. Caulton, M. H. Chisholm, W. E. Streib, Z. Xue, *J. Am. Chem. Soc.* **1991**, *113*, 6082 – 6090; d) Z.-L. Xue, L. A. Morton, *J. Organomet. Chem.* **2011**, *696*, 3924 – 3934.
[6] a) L. A. Morton, X.-H. Zhang, R. Wang, Z. Lin, Y.-D. Wu, Z.-L. Xue, *J. Am. Chem. Soc.* **2004**, *126*, 10208 – 10209; b) P. Chen, B. A. Dougan, X. Zhang, Y.-D. Wu, Z.-L. Xue, *Polyhedron* **2013**, *58*, 30 – 38; c) B. A. Dougan, Z.-L. Xue, *Organometallics* **2009**, *28*, 1295 – 1302; d) L. A. Morton, S. Chen, H. Qiu, Z.-L. Xue, *J. Am. Chem. Soc.* **2007**, *129*, 7277 – 7283.
[7] E. Callens, E. Abou-Hamad, N. Riache, J. M. Basset, *Chem. Commun.* **2014**, *50*, 3982 – 3985.
[8] a) A. Bendjeriou-Sedjerari, J. M. Azzi, E. Abou-Hamad, D. H. Anjum, F. A. Pasha, K.-W. Huang, L. Emsley, J.-M. Basset, *J. Am. Chem. Soc.* **2013**, *135*, 17943 – 17951; b) F. A. Pasha, A. Bendjeriou-Sedjerari, K.-W. Huang, J.-M. Basset, *Organometallics* **2014**, *33*, 3320 – 3327; c) F. A. Pasha, A. Bendjeriou-Sedjerari, E. Abou-Hamad, K.-W. Huang, J.-M. Basset, *Chem. Commun.* **2016**, *52*, 2577 – 2580.
[9] D. F. Schafer, P. T. Wolczanski, E. B. Lobkovsky, *Organometallics* **2011**, *30*, 6539 – 6561.
[10] L. C. H. Gerber, R. R. Schrock, P. Müller, *Organometallics* **2013**, *32*, 2373 – 2378.
[11] a) E. M. Townsend, S. M. Kilyanek, R. R. Schrock, P. Müller, S. J. Smith, A. H. Hoveyda, *Organometallics* **2013**, *32*, 4612 – 4617.

Received: June 19, 2016
Published online: August 11, 2016

